Available online at www.sciencedirect.com
SCIENCE DIRECT®
Journal of Sound and Vibration 287 (2005) 827–843
JOURNAL OF SOUND AND VIBRATION
www.elsevier.com/locate/jsvi

An experimental study of nonlinear oil-film forces of a journal bearing

S.X. Zhao[a,*], X.D. Dai[a], G. Meng[a], J. Zhu[b]

[a]*State Key Laboratory of Vibration, Shock and Noise, Shanghai Jiaotong University, 800 Dongchuan Road, Minhang District, Shanghai 200240, PR China*
[b]*Theory of Lubrication and Bearing Institute, Xi'an Jiaotong University, Xi'an Shannxi 710049, PR China*

Received 13 January 2004; received in revised form 19 July 2004; accepted 13 November 2004
Available online 10 March 2005

Abstract

Hydrodynamic journal bearings under large perturbations go beyond the serviceable range of the linear theory and thus should be treated as nonlinear systems. Three kinds of nonlinear oil-film force models (24-co., 28-co. and 36-co. models) are proposed to denote the oil-film forces by retaining certain terms of Taylor series expansion of the oil-film force. A least-mean squares method in time domain is proposed to identify the oil-film coefficients. The study shows that these three nonlinear models are feasible to describe the oil-film forces and reliable linear oil-film coefficients can be identified from these models.

1. Introduction

Hydrodynamic bearings are generally featured by a set of linear stiffness and damping coefficients in the conventional rotor dynamic models. Theoretically, these coefficients are only valid for small amplitude motion with respect to the equilibrium position. Lund's infinitesimal perturbation method [1] and finite perturbation method are often used to calculate the oil-film coefficients. Qiu and Tieu [2] proved that these two methods predict almost the same results when the perturbation amplitudes are less than $0.02c$ (displacement) or $0.02\omega c$ (velocity) for normal bearing eccentricities; these two results differ by 2.5% if the perturbation amplitude reaches $0.5c$

*Corresponding author. Fax: +86 21 54747451.
E-mail address: zhaosanxing@hotmail.com (S.X. Zhao).

0022-460X/$ - see front matter © 2005 Elsevier Ltd. All rights reserved.
doi:10.1016/j.jsv.2004.11.034

Nomenclature

c radial clearance, mm

$\mathbf{d}_1$ linear damping coefficient matrix

$d_{x,\dot{x}}, d_{x,\dot{y}}, d_{y,\dot{x}}, d_{y,\dot{y}}$ linear damping coefficients, $\mathrm{N\,s\,m^{-1}}$

$D_{X,\dot{X}}, D_{X,\dot{Y}}, D_{Y,\dot{X}}, D_{Y,\dot{Y}}$ dimensionless linear damping coefficients, $D_{i,j} = \frac{d_{i,j}}{\mu L}\left(\frac{c}{R}\right)^3, \quad (i = X \text{ or } Y)$

$\mathbf{d}_2$ second-order damping coefficient matrix

d_2 second-order damping coefficient, $\mathrm{N\,s^2\,m^{-2}}$

D_2 dimensionless second-order damping coefficient, $d_2/D_2 = (1/\omega C)\mu L(R/C)^3$

$\mathbf{d}_3$ third-order damping coefficient matrix

d_3 third-order damping coefficient, $\mathrm{N\,s^3 m^{-3}}$

D_3 dimensionless third-order damping coefficient, $d_3/D_3 = (1/\omega c)^2\mu L(R/c)^3$

$\mathbf{h}_2$ second-order hybrid coefficient matrix

h_2 second-order hybrid coefficient, $\mathrm{N\,s\,m^{-2}}$

H_2 dimensionless second-order hybrid coefficient, $h_2/H_2 = (1/C\mu L(R/C)^3$

f_X, f_Y horizontal and vertical hydrodynamic oil-film forces, N

$F = \frac{f\psi^2}{\mu UL}$ dimensionless force

$\tilde{F}_i$ measured dimensionless dynamic oil-film force (for $i = X$ or Y)

ΔF_i identified dimensionless dynamic oil-film force (for $i = X$ or Y)

f_{x0}, f_{y0} static oil-film forces in the horizontal and vertical direction, N

F_Y load parameter, $f_{Y0}/F_Y = \mu UL/\psi^2$

$\mathbf{k}_1$ linear stiffness coefficient matrix

$k_{x,x}, k_{x,y}, k_{y,x}, k_{y,y}$ linear stiffness coefficients, N/m

$K_{X,X}, K_{X,Y}, K_{Y,X}, K_{Y,Y}$ dimensionless linear stiffness coefficients, $K_{i,j} = \frac{k_{i,j}}{\mu\omega L}\left(\frac{c}{R}\right)^3, \quad (i,j = X, Y)$

$\mathbf{k}_2$ second-order stiffness coefficient matrix

k_2 second-order stiffness coefficient, $\mathrm{N/m^2}$

K_2 dimensionless second-order stiffness coefficient, $k_2/K_2 = (1/C)\mu\omega L(R/C)^3$

$\mathbf{k}_3$ third-order stiffness coefficient matrix

k_3 third-order stiffness coefficient, $\mathrm{N/m^3}$

K_3 dimensionless third-order stiffness coefficient, $k_3/K_3 = (1/C)^2\mu\omega L(R/C)^3$

L bearing length, mm

m mass of bearing housing (including bottom and top splint, four steel robs), Kg

M effective size of data

n journal's rotating speed, rpm

R journal radius, mm

U tangential surface velocity of the journal, $\mathrm{m\,s^{-1}}$

x, y displacements in the horizontal and vertical direction, mm

X, Y dimensionless displacements in the horizontal and vertical direction, $x/X = c$

μ kinetic viscosity, Pa s

ω rotational frequency of the shaft, $\mathrm{rad\,s^{-1}}$

δ dimensionless excitation amplitude

$(\cdot)$ d/dt, derivative with respect to time

Subscripts

X direction of X

Y direction of Y

(displacement) or $0.04\omega c$ (velocity). Hattori [3] analyzed the variations of oil-film stiffness and damping coefficients of a short bearing subjected to large dynamic loads. He concluded that most of the bearing coefficients vary by more than an order of magnitude and the oil-film nonlinearity significantly influences the rotor motion. Muller-Karger and Granados [4] proposed a nonlinear model, in which all terms up to the third-order are retained. Muller-Karger and Barrett [5] studied

the influence of oil-film nonlinearity on the measured dynamic coefficients. They found that the oil-film nonlinearity produced an uncertainty in the coefficients of up to 20 percent compared to the linearized coefficients obtained from a small perturbation solution of the Reynolds equation. Chu and Wood [6] proposed a nonlinear dynamic model taking the higher-order terms into account. In their model, the nonlinearity in the oil-film forces was represented by a set of nonlinear stiffness and damping coefficients, which are functions of static bearing displacement. Choy et al. [7,8] determined the nonlinear stiffness coefficients of the third-, fifth- and seventh-orders at various locations with respect to the equilibrium position. The nonlinearity of the bearing was evaluated by the deviation between the exact stiffness coefficients and the linear coefficients. They concluded that the oil-film nonlinearity is significant and the oil-film forces can be accurately modeled using higher-order stiffness and damping coefficients for displacements far away from the equilibrium position.

Accordingly, nonlinear oil-film forces are much more complicated than linear forces. The study on nonlinear oil-film forces is still rare and most papers are confined to theoretical analyses. The purpose of this paper is to derive some new nonlinear oil-film force models and to identify these dynamic coefficients based on the experimental data.

2. Nonlinear oil-film force models

Linear oil-film coefficients with respect to an equilibrium position of the journal are inaccurate when the bearing system vibrates with large amplitudes due to a dynamic load. In this case, the high-order terms of the Taylor series expansion of oil-film forces should be retained. Bearing oil-film forces will become nonlinear functions of the journal's displacement and velocity. Using the second-order Taylor series expansion, bearing oil-film forces can be written as

$$f_i = f_{i0} + \frac{1}{1!}\left(x\frac{\partial}{\partial x} + y\frac{\partial}{\partial y} + \dot{x}\frac{\partial}{\partial \dot{x}} + \dot{y}\frac{\partial}{\partial \dot{y}}\right) f_i(x_0, y_0, 0, 0) + \frac{1}{2!}\left(x\frac{\partial}{\partial x} + y\frac{\partial}{\partial y} + \dot{x}\frac{\partial}{\partial \dot{x}} + \dot{y}\frac{\partial}{\partial \dot{y}}\right)^2 f_i(x_0, y_0, 0, 0), \quad (i = x \text{ or } y) \tag{1}$$

where $(x_0, y_0, 0, 0)$ represents the static equilibrium position of the journal, x and y are the journal's relative movement coordinates in the X and Y directions.

It can be seen that the oil-film forces have 14 dynamic coefficients in the horizontal (X) and vertical (Y) direction, respectively. These coefficients include the linear stiffness and damping coefficients, the second-order stiffness and damping coefficients, and the second-order hybrid coefficients. They are involved in the following matrices:

$$\mathbf{k}_1 = \begin{bmatrix} k_{x,x} & k_{x,y} \\ k_{y,x} & k_{y,y} \end{bmatrix} = \begin{bmatrix} \left.\frac{\partial f_x}{\partial x}\right|_{(x_0,y_0,0,0)} & \left.\frac{\partial f_x}{\partial y}\right|_{(x_0,y_0,0,0)} \\ \left.\frac{\partial f_y}{\partial x}\right|_{(x_0,y_0,0,0)} & \left.\frac{\partial f_y}{\partial y}\right|_{(x_0,y_0,0,0)} \end{bmatrix},$$

$$\mathbf{d}_1 = \begin{bmatrix} d_{x,\dot{x}} & d_{x,\dot{y}} \\ d_{y,\dot{x}} & d_{y,\dot{y}} \end{bmatrix} = \begin{bmatrix} \left.\frac{\partial f_x}{\partial \dot{x}}\right|_{(x_0,y_0,0,0)} & \left.\frac{\partial f_x}{\partial \dot{y}}\right|_{(x_0,y_0,0,0)} \\ \left.\frac{\partial f_y}{\partial \dot{x}}\right|_{(x_0,y_0,0,0)} & \left.\frac{\partial f_y}{\partial \dot{y}}\right|_{(x_0,y_0,0,0)} \end{bmatrix},$$

$$\mathbf{k}_2 = \begin{bmatrix} k_{x,x^2} & k_{x,y^2} & k_{x,xy} \\ k_{y,x^2} & k_{y,y^2} & k_{y,xy} \end{bmatrix} = \begin{bmatrix} \left.\frac{1}{2}\frac{\partial^2 f_x}{\partial x^2}\right|_{(x_0,y_0,0,0)} & \left.\frac{1}{2}\frac{\partial^2 f_x}{\partial y^2}\right|_{(x_0,y_0,0,0)} & \left.\frac{\partial^2 f_x}{\partial x \partial y}\right|_{(x_0,y_0,0,0)} \\ \left.\frac{1}{2}\frac{\partial^2 f_y}{\partial x^2}\right|_{(x_0,y_0,0,0)} & \left.\frac{1}{2}\frac{\partial^2 f_y}{\partial y^2}\right|_{(x_0,y_0,0,0)} & \left.\frac{\partial^2 f_y}{\partial x \partial y}\right|_{(x_0,y_0,0,0)} \end{bmatrix},$$

$$\mathbf{d}_2 = \begin{bmatrix} d_{x,\dot{x}^2} & d_{x,\dot{y}^2} & d_{x,\dot{x}\dot{y}} \\ d_{y,\dot{x}^2} & d_{y,\dot{y}^2} & d_{x,\dot{x}\dot{y}} \end{bmatrix} = \begin{bmatrix} \left.\frac{1}{2}\frac{\partial^2 f_x}{\partial \dot{x}^2}\right|_{(x_0,y_0,0,0)} & \left.\frac{1}{2}\frac{\partial^2 f_x}{\partial \dot{y}^2}\right|_{(x_0,y_0,0,0)} & \left.\frac{\partial^2 f_x}{\partial \dot{x} \partial \dot{y}}\right|_{(x_0,y_0,0,0)} \\ \left.\frac{1}{2}\frac{\partial^2 f_y}{\partial \dot{x}^2}\right|_{(x_0,y_0,0,0)} & \left.\frac{1}{2}\frac{\partial^2 f_y}{\partial \dot{y}^2}\right|_{(x_0,y_0,0,0)} & \left.\frac{\partial^2 f_y}{\partial \dot{x} \partial \dot{y}}\right|_{(x_0,y_0,0,0)} \end{bmatrix},$$

$$\mathbf{h}_2 = \begin{bmatrix} h_{x,x\dot{x}} & h_{x,x\dot{y}} & h_{x,y\dot{x}} & h_{x,y\dot{y}} \\ h_{y,x\dot{x}} & h_{y,x\dot{y}} & h_{y,y\dot{x}} & h_{y,y\dot{y}} \end{bmatrix} = \begin{bmatrix} \left.\frac{\partial^2 f_x}{\partial x \partial \dot{x}}\right|_{(x_0,y_0,0,0)} & \left.\frac{\partial^2 f_x}{\partial x \partial \dot{y}}\right|_{(x_0,y_0,0,0)} & \left.\frac{\partial^2 f_x}{\partial y \partial \dot{x}}\right|_{(x_0,y_0,0,0)} & \left.\frac{\partial^2 f_x}{\partial y \partial \dot{y}}\right|_{(x_0,y_0,0,0)} \\ \left.\frac{\partial^2 f_y}{\partial x \partial \dot{x}}\right|_{(x_0,y_0,0,0)} & \left.\frac{\partial^2 f_y}{\partial x \partial \dot{y}}\right|_{(x_0,y_0,0,0)} & \left.\frac{\partial^2 f_y}{\partial y \partial \dot{x}}\right|_{(x_0,y_0,0,0)} & \left.\frac{\partial^2 f_y}{\partial y \partial \dot{y}}\right|_{(x_0,y_0,0,0)} \end{bmatrix},$$

where $\mathbf{k}_1$ and $\mathbf{d}_1$ are the linear stiffness and damping coefficient matrices; $\mathbf{k}_2$ and $\mathbf{d}_2$ are the second-order stiffness and damping coefficient matrices; $\mathbf{h}_2$ is the second-order hybrid coefficient matrix.

Combining Eq. (1) and the aforementioned matrices, the dynamic oil-film forces can be modeled as

$$\begin{bmatrix} \Delta f_x \\ \Delta f_y \end{bmatrix} = \mathbf{k}_1 \begin{bmatrix} x \\ y \end{bmatrix} + \mathbf{d}_1 \begin{bmatrix} \dot{x} \\ \dot{y} \end{bmatrix} + \mathbf{k}_2 \begin{bmatrix} x^2 \\ y^2 \\ xy \end{bmatrix} + \mathbf{d}_2 \begin{bmatrix} \dot{x}^2 \\ \dot{y}^2 \\ \dot{x}\dot{y} \end{bmatrix} + \mathbf{h}_2 \begin{bmatrix} x\dot{x} \\ x\dot{y} \\ y\dot{x} \\ y\dot{y} \end{bmatrix}. \tag{2}$$

As shown in Eq. (2), the nonlinear oil-film force model is much more complicated than the linear oil-film force model due to more coefficients involved. For example, the nonlinear model will have 28, 68 and 138 oil-film coefficients if the Taylor series expansion is retained to the second-, third- and fourth-order terms, respectively. In fact, the model can be conveniently represented by some of these nonlinear terms. The order of the expression can be adjusted through the truncation error depending on the practical application. In this paper, there are seven kinds of oil-film coefficients to be considered. They are (1) the linear stiffness coefficient k; (2) the linear damping coefficient d; (3) the second-order stiffness coefficient k_2; (4) the second-order damping coefficient d_2; (5) the second-order hybrid coefficient h_2; (6) the third-order stiffness coefficient k_3; and (7) the third-order damping coefficient d_3. Three models, which retain different oil-film coefficients, are studied in the following sections.

2.1. 28-coefficient oil-film force model (28-co. model)

When all terms in the second-order Taylor series expansion are retained, the nonlinear oil-film force model has 28 coefficients in all. Using dimensionless coefficients $K_{i,j}$ (for $i = X$ or Y, and $j = 1-14$), the (dimensionless) dynamic oil-film force can be simplified as

$$\Delta F_i = K_{i,1}\cdot X + K_{i,2}\cdot Y + K_{i,3}\cdot \dot{X} + K_{i,4}\cdot \dot{Y} + K_{i,5}\cdot X^2 + K_{i,6}\cdot XY + K_{i,7}\cdot X\dot{X} + K_{i,8}\cdot X\dot{Y} + K_{i,9}\cdot Y^2 + K_{i,10}\cdot Y\dot{X} + K_{i,11}\cdot Y\dot{Y} + K_{i,12}\cdot \dot{X}^2 + K_{i,13}\cdot \dot{X}\dot{Y} + K_{i,14}\cdot \dot{Y}^2, \quad (3)$$

where $K_{i,1}$ and $K_{i,2}$ are linear stiffness coefficients; $K_{i,3}$ and $K_{i,4}$ are linear damping coefficients; $K_{i,5}, K_{i,6}$ and $K_{i,9}$ are second-order stiffness coefficients; $K_{i,12}, K_{i,13}$ and $K_{i,14}$ are second-order damping coefficients; $K_{i,7}, K_{i,8}, K_{i,10}$ and $K_{i,11}$ are second-order hybrid coefficients.

2.2. 24-coefficient oil-film force model (24-co. model)

When the third-order Taylor series expansion only retains terms associated with direct stiffness and damping coefficients, the nonlinear oil-film force model has 24 coefficients in all. Then, the dynamic oil-film force can be described as ($i = X$ or Y)

$$\Delta F_i = K_{i,1}\cdot X + K_{i,2}\cdot Y + K_{i,3}\cdot \dot{X} + K_{i,4}\cdot \dot{Y} + K_{i,5}\cdot X^2 + K_{i,6}\cdot Y^2 + K_{i,7}\cdot \dot{X}^2 + K_{i,8}\cdot \dot{Y}^2 + K_{i,9}\cdot X^3 + K_{i,10}\cdot Y^3 + K_{i,11}\cdot \dot{X}^3 + K_{i,12}\cdot \dot{Y}^3, \quad (4)$$

where $K_{i,1}$ and $K_{i,2}$ are linear stiffness coefficients; $K_{i,3}$ and $K_{i,4}$ are linear damping coefficients; $K_{i,5}$ and $K_{i,6}$ are second-order stiffness coefficients; $K_{i,7}$ and $K_{i,8}$ are second-order damping coefficients; $K_{i,9}$ and $K_{i,10}$ are third-order stiffness coefficients; and $K_{i,11}$ and $K_{i,12}$ are third-order damping coefficients.

2.3. 36-coefficient oil-film force model (36-co. model)

When the Taylor series expansion retains all terms up to the second-order and the terms associated with third-order direct stiffness and damping coefficients, the nonlinear oil-film force model has 36 coefficients in all. Accordingly, the dynamic oil-film forces can be written as ($i = X$ or Y)

$$\Delta F_i = K_{i,1}\cdot X + K_{i,2}\cdot Y + K_{i,3}\cdot \dot{X} + K_{i,4}\cdot \dot{Y} + K_{i,5}\cdot X^2 + K_{i,6}\cdot XY + K_{i,7}\cdot X\dot{X} + K_{i,8}\cdot X\dot{Y} + K_{i,9}\cdot Y^2 + K_{i,10}\cdot Y\dot{X} + K_{i,11}\cdot Y\dot{Y} + K_{i,12}\cdot \dot{X}^2 + K_{i,13}\cdot \dot{X}\dot{Y} + K_{i,14}\cdot \dot{Y}^2 + K_{i,15}\cdot X^3 + K_{i,16}\cdot Y^3 + K_{i,17}\cdot \dot{X}^3 + K_{i,18}\cdot \dot{Y}^3, \quad (5)$$

where coefficients $K_{i,1}$–$K_{i,14}$ have the same meanings as those in Eq. (3), $K_{i,15}$ and $K_{i,16}$ are third-order stiffness coefficients, $K_{i,17}$ and $K_{i,18}$ are third-order damping coefficients.

3. Identification of oil-film dynamic coefficients

Using the multi-frequency identification method [9] to the experimental data obtained from a test rig (its details have been presented in Ref. [9]), a set of discrete values in time domain about $X(k), Y(k), \dot{X}(k), \dot{Y}(k), \tilde{F}_X(k)$ and $\tilde{F}_Y(k)(k = 1-M)$ can be achieved. The oil-film dynamic coefficients can be identified using the least-mean-square method.

The least mean square between the measured dynamic oil-film force $\tilde{F}_i(k)$ and the identified force $\Delta F_i(k)$ (modeled by Eqs. (3)–(5)) can be calculated as follows ($i = X$ or Y, and $j = 1-12, 14$ or 18)

$$\min_{(K_{i,j})} \varepsilon_i^2 = \sum_{k=1}^{M} [\tilde{F}_i(k) - \Delta F_i(k)]^2. \tag{6}$$

Then the following equation can be deduced (for 28-co. model):

$$\frac{\partial \varepsilon_i^2}{\partial K_{i,p}} = 0 \quad (p = 1-14; \;\; i = X, Y). \tag{7}$$

Substituting Eq. (3) into Eq. (7) yields

$$\begin{bmatrix} \sum_{k=1}^{M} X(k)^2 & \sum_{k=1}^{M} X(k)Y(k) & \cdots & \sum_{k=1}^{M} X(k)\dot{X}(k)\dot{Y}(k) & \sum_{k=1}^{M} X(k)\dot{Y}(k)^2 \\ \sum_{k=1}^{M} Y(k)X(k) & \sum_{k=1}^{M} Y(k)^2 & \cdots & \sum_{k=1}^{M} Y(k)\dot{X}(k)\dot{Y}(k) & \sum_{k=1}^{M} Y(k)\dot{Y}(k)^2 \\ \vdots & \vdots & \ddots & \vdots & \vdots \\ \sum_{k=1}^{M} \dot{X}(k)\dot{Y}(k)X(k) & \sum_{k=1}^{M} \dot{X}(k)\dot{Y}(k)Y(k) & \cdots & \sum_{k=1}^{M} \dot{X}(k)^2\dot{Y}(k)^2 & \sum_{k=1}^{M} \dot{X}(k)\dot{Y}(k)^3 \\ \sum_{k=1}^{M} \dot{Y}(k)^2X(k) & \sum_{k=1}^{M} \dot{Y}(k)^2Y(k) & \cdots & \sum_{k=1}^{M} \dot{Y}(k)^3\dot{X}(k) & \sum_{k=1}^{M} \dot{Y}(k)^4 \end{bmatrix}_{14\times 14} \mathbf{X}$$

$$= \begin{bmatrix} \sum_{k=1}^{M} X(k)\tilde{F}_i(k) \\ \sum_{k=1}^{M} Y(k)\tilde{F}_i(k) \\ \vdots \\ \sum_{k=1}^{M} \dot{X}(k)\dot{Y}(k)\tilde{F}_i(k) \\ \sum_{k=1}^{M} \dot{Y}(k)^2\tilde{F}_i(k) \end{bmatrix}_{14\times 1}, \tag{8}$$

where $\mathbf{X} = [K_{i1}, K_{i2}, K_{i3}, K_{i4}, K_{i5}, K_{i6}, K_{i7}, K_{i8}, K_{i9}, K_{i,10}, K_{i,11}, K_{i,12}, K_{i,13}, K_{i,14}]^{\mathrm{T}}$. Fig. 1 plots the measured and identified dynamic oil-film forces according to a set of experimental data. It can be seen that the identified dynamic oil-film forces match the measured data very well. The difference between the identified force $\Delta F_i(k)$ and the measured force $\tilde{F}_i(k)$ can be evaluated by the coefficient of determination (COD), which is defined as follows:

$$\mathrm{COD} = 1 - \frac{\sum(\tilde{F}(k) - \Delta F(k))^2}{\sum(\tilde{F}(k) - \bar{F})^2}, \tag{9}$$

where $\bar{F}$ is the mean value of $\tilde{F}(k)$. The COD is a well-known indicator to evaluate the difference between the proposed model and its corresponding experimental data. Note that the value of COD is between 0 and 1 with 1 indicating the perfect matching. Calculations show that COD values for the nonlinear oil-film force model are 0.9979 in the X direction and 0.9977 in the Y direction. Therefore, the nonlinear model is feasible to describe the oil-film forces.

Eq. (8) is used to identify the 28-co. model. Likewise, the 24-co. model and the 36-co. model can also be identified when proper equations are employed.

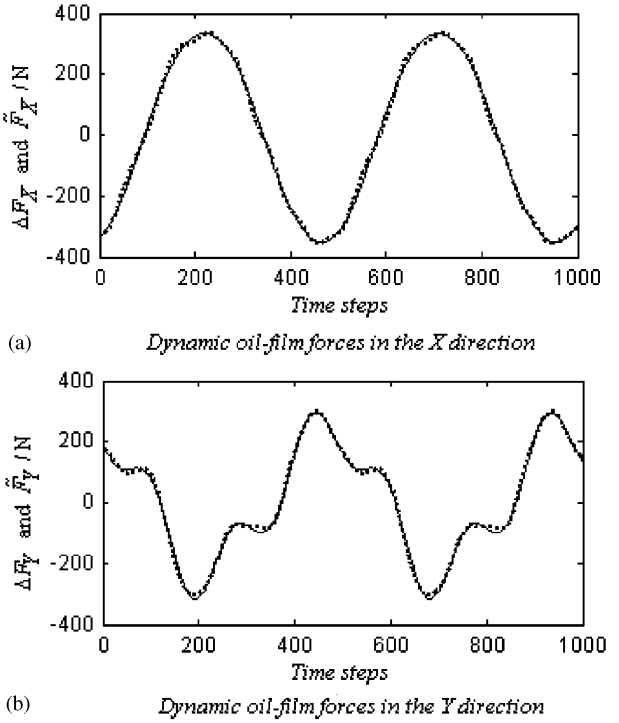

Fig. 1. Measured and identified dynamic oil-film forces in the X and Y directions. Measured oil-film forces $\tilde{F}_i$: —; identified oil-film forces ΔF_i: . . . .

For the 24-co. model,

$$\begin{bmatrix} \sum_{k=1}^{M} X(k)^2 & \sum_{k=1}^{M} X(k)Y(k) & \cdots & \sum_{k=1}^{M} X(k)\dot{X}(k)^3 & \sum_{k=1}^{M} X(k)\dot{Y}(k)^3 \\ \sum_{k=1}^{M} Y(k)X(k) & \sum_{k=1}^{M} Y(k)^2 & \cdots & \sum_{k=1}^{M} Y(k)\dot{X}(k)^3 & \sum_{k=1}^{M} Y(k)\dot{Y}(k)^3 \\ \vdots & \vdots & \ddots & \vdots & \vdots \\ \sum_{k=1}^{M} \dot{X}(k)^3X(k) & \sum_{k=1}^{M} \dot{X}(k)^3Y(k) & \cdots & \sum_{k=1}^{M} \dot{X}(k)^6 & \sum_{k=1}^{M} \dot{X}(k)^3Y(k)^3 \\ \sum_{k=1}^{M} \dot{Y}(k)^3X(k) & \sum_{k=1}^{M} \dot{Y}(k)^3Y(k) & \cdots & \sum_{k=1}^{M} \dot{Y}(k)^3\dot{X}(k)^3 & \sum_{k=1}^{M} \dot{Y}(k)^6 \end{bmatrix}_{12\times 12} \mathbf{X}$$

$$= \begin{bmatrix} \sum_{k=1}^{M} X(k)\tilde{F}_i(k) \\ \sum_{k=1}^{M} Y(k)\tilde{F}_i(k) \\ \vdots \\ \sum_{k=1}^{M} \dot{X}(k)^3\tilde{F}_i(k) \\ \sum_{k=1}^{M} \dot{Y}(k)^3\tilde{F}_i(k) \end{bmatrix}_{12\times 1}. \tag{10}$$

For the 36-co. model,

$$\begin{bmatrix} \sum_{k=1}^{M} X(k)^2 & \sum_{k=1}^{M} X(k)Y(k) & \cdots & \sum_{k=1}^{M} X(k)\dot{X}(k)^3 & \sum_{k=1}^{M} X(k)\dot{Y}(k)^3 \\ \sum_{k=1}^{M} Y(k)X(k) & \sum_{k=1}^{M} Y(k)^2 & \cdots & \sum_{k=1}^{M} Y(k)\dot{X}(k)^3 & \sum_{k=1}^{M} Y(k)\dot{Y}(k)^3 \\ \vdots & \vdots & \ddots & \vdots & \vdots \\ \sum_{k=1}^{M} \dot{X}(k)^3X(k) & \sum_{k=1}^{M} \dot{X}(k)^3Y(k) & \cdots & \sum_{k=1}^{M} \dot{X}(k)^6 & \sum_{k=1}^{M} \dot{X}(k)^3\dot{Y}(k)^3 \\ \sum_{k=1}^{M} \dot{Y}(k)^3X(k) & \sum_{k=1}^{M} \dot{Y}(k)^3Y(k) & \cdots & \sum_{k=1}^{M} \dot{Y}(k)^3\dot{X}(k)^3 & \sum_{k=1}^{M} \dot{Y}(k)^6 \end{bmatrix}_{18\times 18} \mathbf{X}$$

$$= \begin{bmatrix} \sum_{k=1}^{M} X(k)\tilde{F}_i(k) \\ \sum_{k=1}^{M} Y(k)\tilde{F}_i(k) \\ \vdots \\ \sum_{k=1}^{M} \dot{X}(k)^3\tilde{F}_i(k) \\ \sum_{k=1}^{M} \dot{Y}(k)^3\tilde{F}_i(k) \end{bmatrix}_{18\times 1} . \tag{11}$$

4. Results and discussion

4.1. Comparisons between the linear oil-film force model and nonlinear models

Based on a set of experimental data, four sets of oil-film coefficients, which are associated with the linear and nonlinear oil-film force models, can be identified. Tables 1 and 2 list all the oil-film coefficients in the X and Y directions. The experiment was conducted when $n = 1250\,\text{rpm}, F_Y = 0.6396$, and the maximum excitation amplitude $0.025c$ ($\delta = 0.025$).

As shown in Tables 1 and 2, the identified linear coefficients using these three nonlinear models are similar to each other. However, they are quite different from those obtained from the linear model. The identified nonlinear coefficients using these three nonlinear models are different to some extent. Some of the coefficients are similar to each other, while others exhibit great disagreements. Fig. 2 shows the measured dynamic oil-film forces and the identified forces. Here, the 28-co. model and the linear model have been used, respectively. It indicates that the 28-co. model is in good agreement with the experimental data, while the linear model has some discrepancies. Further investigation shows that the 24-co. model and 36-co. model well coincide with the experimental data (each of CODs in the X an Y directions for these nonlinear models are larger than 0.99), thus they are also suitable to describe the dynamic oil-film forces.

When $n = 1250\,\text{rpm}$ and $F_Y = 0.6396$, multi-sets of experimental data with various excitation amplitudes have been achieved. Based on these sets of experimental data, the linear oil-film force model and nonlinear oil-film force models can be identified. Fig. 3 presents the COD values for the linear model and the 28-co. model with respect to the excitation amplitude. It indicates that the COD values for the nonlinear oil-film force model are close to 1 in both of the X and Y direction. It can also be observed that the COD values for the linear model decrease when the excitation amplitude increases. Therefore, the linear oil-film force model becomes invalid when the amplitude excitation increases. Nevertheless, the nonlinear oil-film force model still works well with large excitation amplitudes.

Table 1
Dynamic coefficients in the X direction, $F_Y = 0.6396$, $n = 1250$ rpm, $\delta = 0.025$

Model	$K_{X,X}$	$K_{X,Y}$	$D_{X,\dot{X}}$	$D_{X,\dot{Y}}$	K_{X,X^2}	$K_{X,XY}$	$H_{X,X\dot{X}}$	$H_{X,X\dot{Y}}$	K_{X,Y^2}	$H_{X,Y\dot{X}}$	$H_{X,Y\dot{Y}}$	$D_{X,\dot{X}^2}$	$D_{X,\dot{X}\dot{Y}}$	$D_{X,\dot{Y}^2}$	K_{X,X^3}	K_{X,Y^3}	$D_{X,\dot{X}^3}$	$D_{X,\dot{Y}^3}$
LM[a]	0.6802	−0.6669	1.3580	0.6017	—	—	—	—	—	—	—	—	—	—	—	—	—	—
24-Co.	0.8908	−0.0277	0.5462	0.6526	−1.3043	—	—	—	−0.7488	—	—	0.8144	—	0.4862	−28.665	20.821	2.3306	−10.129
28-Co.	0.8517	−0.0455	0.5462	0.6048	−4.1484	0.6218	−6.0160	−20.810	−2.2998	5.7881	1.8901	−5.0836	−17.790	−25.620	—	—	—	—
36-Co.	0.8507	−0.0470	0.5466	0.6048	−3.5177	0.7977	−5.6454	−19.158	−2.6745	6.4787	2.5727	−5.3012	−17.707	−24.691	1.0794	4.4230	6.1598	−24.089

[a]LM—linear model.

Table 2
Dynamic coefficients in the Y direction, $F_Y = 0.6396$, $n = 1250$ rpm, $\delta = 0.025$

Model	$K_{Y,X}$	$K_{Y,Y}$	$D_{Y,\dot{X}}$	$D_{Y,\dot{Y}}$	K_{Y,X^2}	$K_{Y,XY}$	$H_{Y,X\dot{X}}$	$H_{Y,X\dot{Y}}$	K_{Y,Y^2}	$H_{Y,Y\dot{X}}$	$H_{Y,Y\dot{Y}}$	$D_{Y,\dot{X}^2}$	$D_{Y,\dot{X}\dot{Y}}$	$D_{Y,\dot{Y}^2}$	K_{Y,X^3}	K_{Y,Y^3}	$D_{Y,\dot{X}^3}$	$D_{Y,\dot{Y}^3}$
LM[a]	2.7026	0.9194	1.0664	5.5903	—	—	—	—	—	—	—	—	—	—	—	—	—	—
24-Co.	1.4035	1.6953	0.2217	1.5282	1.8437	—	—	—	1.5957	—	—	1.5263	—	5.4077	−10.887	−22.165	−4.5632	113.16
28-Co.	1.5969	1.7290	0.2716	1.7965	35.092	5.8955	46.9025	137.197	5.6048	−12.250	12.377	26.710	92.125	137.62	—	—	—	—
36-Co.	1.6017	1.7340	0.2698	1.7995	32.294	6.2588	44.1045	129.205	6.8232	−14.117	11.649	26.893	89.270	132.32	99.456	−133.79	4.4646	6.1972

[a]LM—linear model.

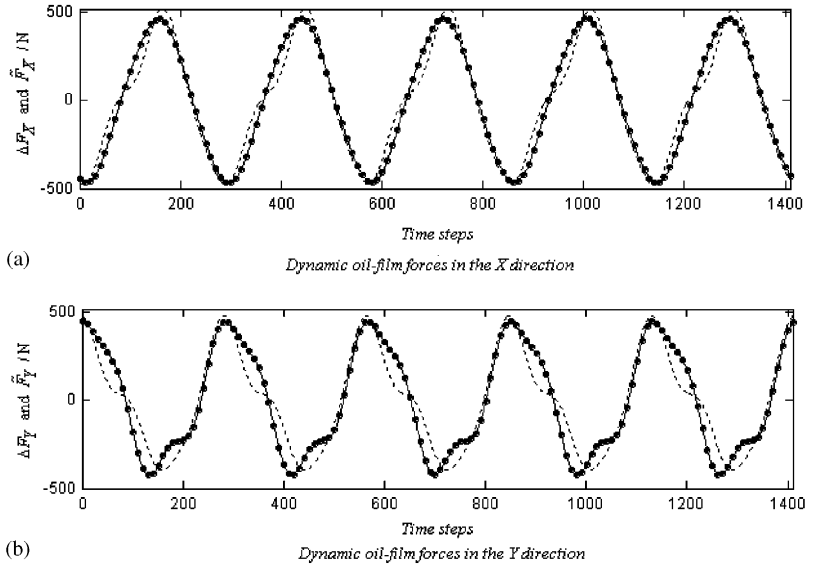

Fig. 2. Measured and identified dynamic oil-film forces in the X and Y directions ($F_Y = 0.6396$, $n = 1250$ rpm, $\delta = 0.15$). Measured: —; linear model: ...; nonlinear model (28-co. model): •.

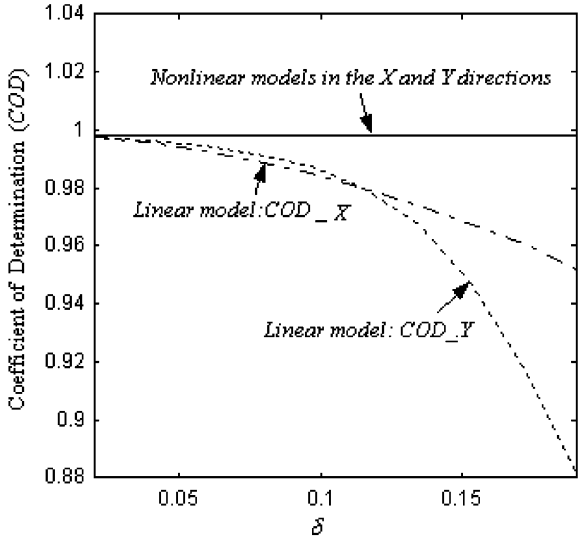

Fig. 3. CODs vs. dimensionless excitation amplitude δ ($F_Y = 0.6396$, $n = 1250$ rpm).

4.2. Comparisons between the identified oil-film coefficients

In this section, the identified coefficients obtained from different oil-film force models will be compared and the influence of excitation amplitude on the identified coefficients will be further discussed. Figs. 4 and 5 plot the variations of identified linear stiffness and damping coefficients with respect to excitation amplitude. The experiments were conducted when $F_Y = 0.7750$ and

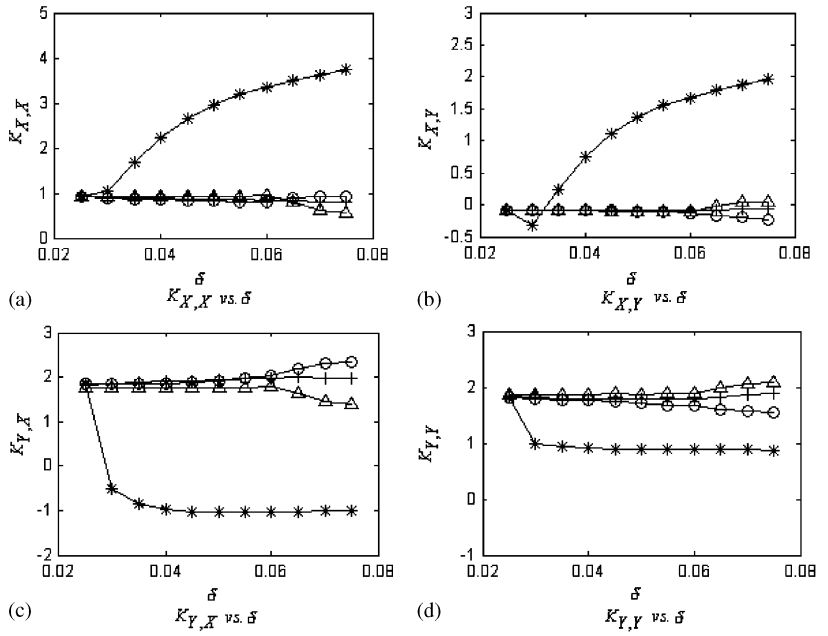

Fig. 4. Identified linear stiffness coefficients vs. dimensionless excitation amplitude δ ($F_Y = 0.7750$, $n = 1250$ rpm). Linear model: $*$; 24-co. model: $\circ$; 28-co. model: $+$; 36-co. model: $\triangle$.

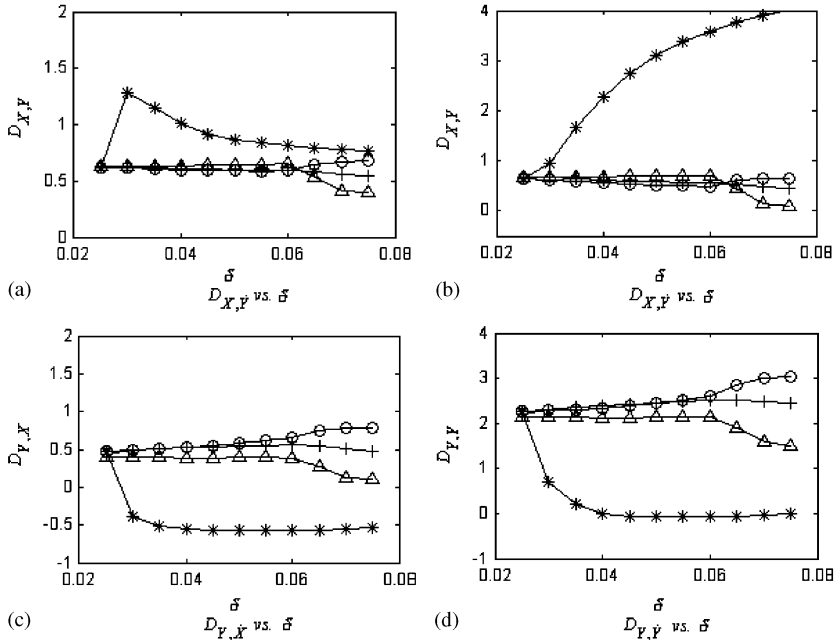

Fig. 5. Identified linear damping coefficients vs. dimensionless excitation amplitude δ ($F_Y = 0.7750$, $n = 1250$ rpm). Linear model: $*$; 24-co. model: $\circ$; 28-co. model: $+$; 36-co. model: $\triangle$.

$n = 1250$ rpm. It shows that the identified linear stiffness and damping coefficients obtained from these nonlinear models are consistent and close to each other when the excitation amplitude is less than $0.06c$. However, the identified linear stiffness and damping coefficients obtained from the linear model are sensitive to the excitation amplitude. Only when the excitation amplitude is small enough ($\delta \leqslant 0.025$), the linear model can receive the similar results with these nonlinear models.

Nonlinear stiffness and damping coefficients obtained from these nonlinear models are illustrated in Figs. 6–9. For the sake of simplicity, only a part of nonlinear coefficients (i.e., the second-order stiffness coefficients K_{X,X^2} and K_{X,Y^2}; the second-order damping coefficients $D_{X,\dot{X}^2}$ and $D_{X,\dot{Y}^2}$; the third-order stiffness coefficients $K_{X,X^3}, K_{X,Y^3}, K_{Y,X^3}$ and K_{Y,Y^3}; and the third-order damping coefficients $D_{X,\dot{X}^3}, D_{X,\dot{Y}^3}, D_{Y,\dot{X}^3}$ and $D_{Y,\dot{Y}^3}$) are presented. It should be noted that these four figures correspond to different operational conditions. For Figs. 6 and 7, $F_Y = 0.7750$ and $n = 1250$ rpm; and for Figs. 8 and 9, $F_Y = 0.6396$ and $n = 1250$ rpm.

It can be seen from Figs. 6 and 7 that the 24-co. model can receive stable second-order oil-film coefficients, while the other two nonlinear models cannot receive stable results. It should be noted that the identified nonlinear coefficients from 24-co. model in Fig. 6 are close to those in Fig. 7. The reason for this phenomenon is that the load parameters corresponding to these two figures are approximate (Fig. 6: $F_Y = 0.7750$, Fig. 7: $F_Y = 0.6396$).

Figs. 8 and 9 depict the identified third-order stiffness and damping coefficients, which are received from two nonlinear models (24-co. model and 36-co. model). It can be found that the identified third-order oil-film coefficients are not consistent and change with the excitation amplitude. What is more from Figs. 8 and 9, the identified third-order oil-film coefficients will

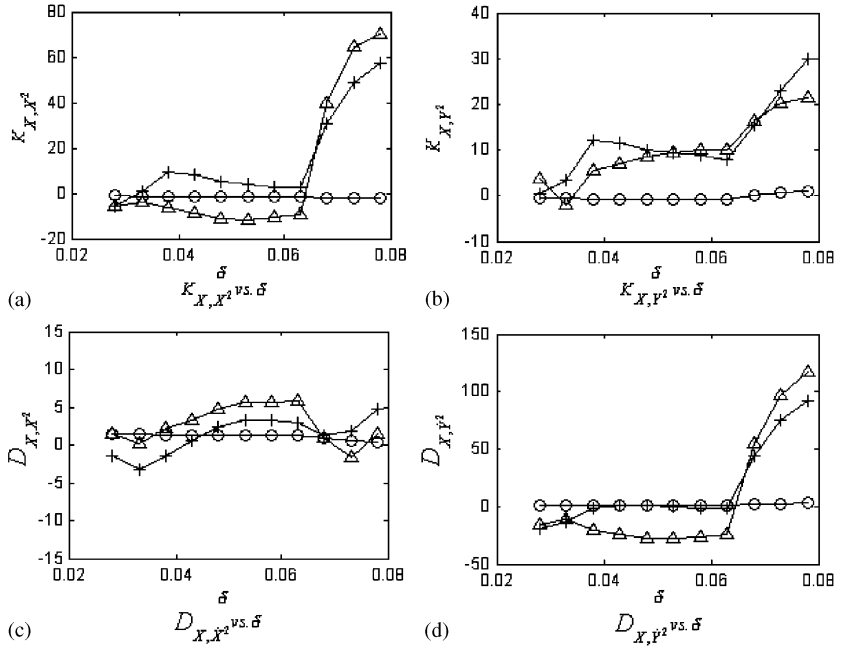

Fig. 6. Identified second-order stiffness and damping coefficients vs. dimensionless excitation amplitude δ ($F_Y = 0.7750$, $n = 1250$ rpm). 24-co. model: ○; 28-co. model: +; 36-co. model: △.

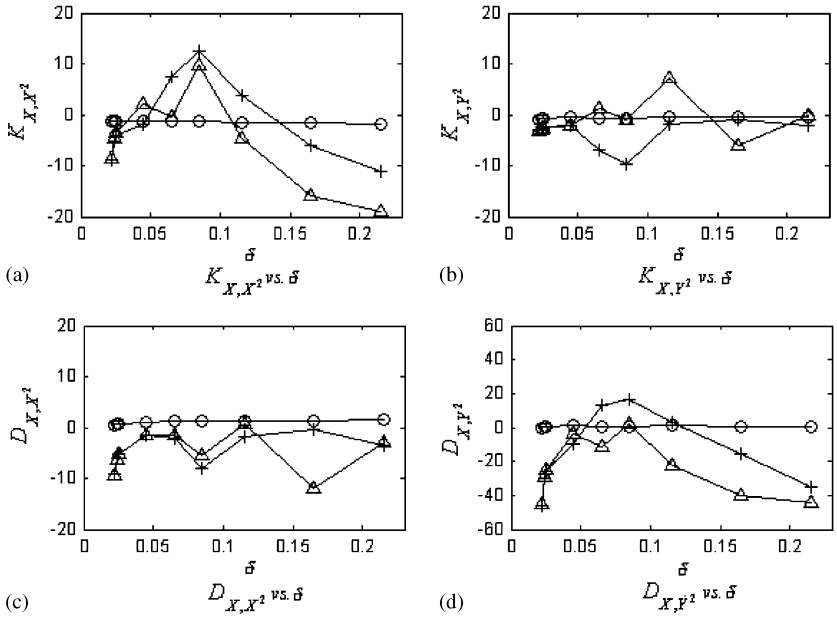

Fig. 7. Identified second-order stiffness and damping coefficients vs. dimensionless excitation amplituded δ ($F_Y = 0.6396$, $n = 1250$ rpm). 24-co. model: ○; 28-co. model: +; 36-co. model: △.

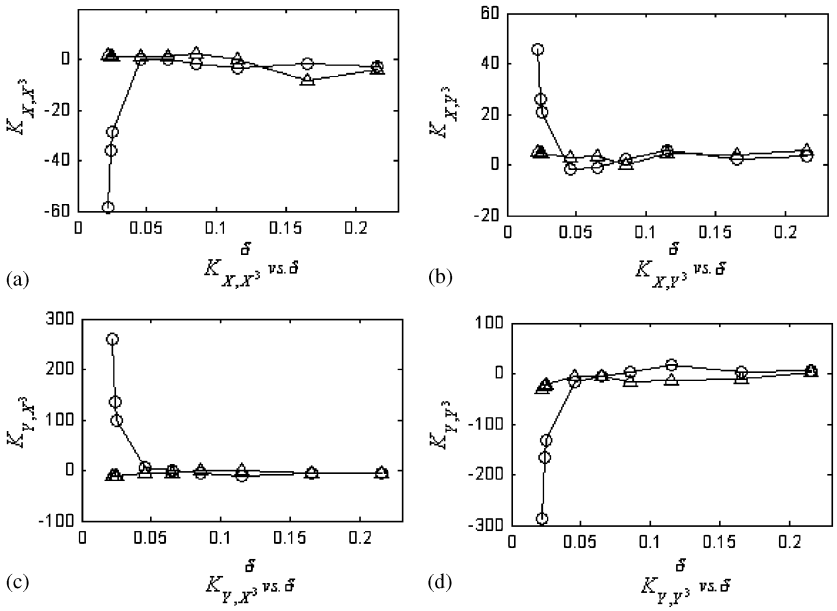

Fig. 8. Identified third-order stiffness coefficients vs. dimensionless excitation amplitude δ ($F_Y = 0.6396$, $n = 1250$ rpm). 24-co. model: ○; 36-co. model: △.

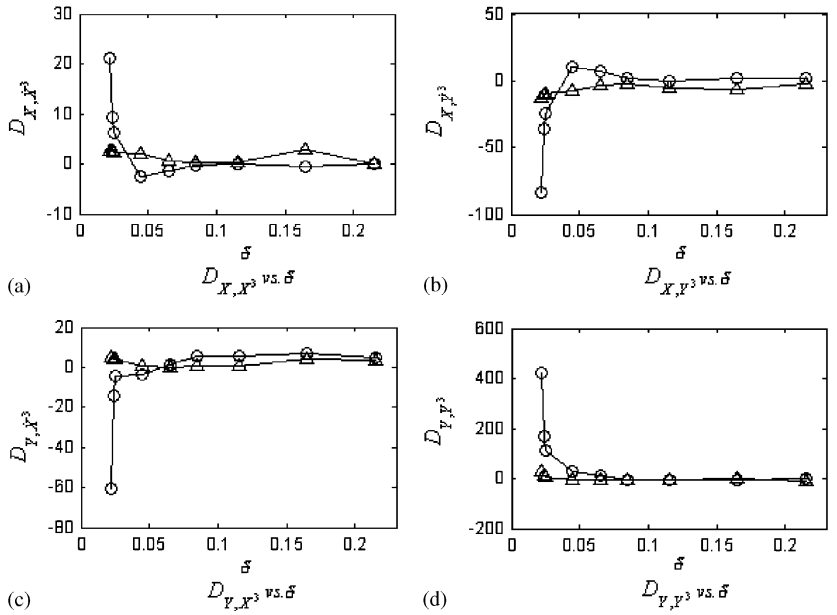

Fig. 9. Identified third-order damping coefficients vs. dimensionless excitation amplitude δ ($F_Y = 0.6396$, $n =$ 1250 rpm). 24-co. model: ○; 36-co. model: △.

remain constant when the excitation amplitude is large enough. So the stable third-order oil-film coefficients may be obtained from these two nonlinear models as long as the excitation amplitude is large enough.

In general, reliable linear oil-film coefficients can be received from these three nonlinear models, while stable nonlinear coefficients cannot be obtained from these nonlinear models except for some second-order oil-film coefficients, which can be received from the 24-co. model. The following are some reasons for these phenomena.

The reason why it is difficult to receive stable nonlinear coefficients is that Eqs. (8), (10) and (11) are ill-conditioned system of equations. But it is strange that reliable linear coefficients can still be received from these nonlinear models. These phenomena may be a result of the coefficient matrices of Eqs. (8), (10) and (11).

These coefficient matrices are diagonal-dominant and positive definite Hermitian matrices. The diagonal elements in these coefficient matrices compose an approximate descending sequence, and besides, they play a dominant role in identifying oil-film coefficients. Taking the 36-co. model for example (the coefficient matrix is 18×18), the diagonal element sequence according to a set of experimental data ($F_Y = 0.6396, n = 1250\,\text{rpm}, \delta = 0.025$) is following:

$$\{86, 38, 6.4, 3.5, 6.6, 2, 0.35, 0.19, 1.3, 0.18, 0.08, 0.05, 0.03, 0.02, 0.57, 0.053, 0.0004, 0.0002\}.$$

It can be seen that the latter diagonal elements of the coefficients matrix are very small, while the former diagonal elements are rather large. Because the latter diagonal elements have greater effect on the nonlinear coefficients than on the linear coefficients, the identified nonlinear coefficients are

more sensitive to the testing errors. That is why reliable nonlinear coefficients cannot be obtained from 36-co. model in the case of ordinary excitation amplitude. Meanwhile, since the former diagonal elements are large, stable linear coefficients can be received. This is a typical case in identifying the oil-film coefficients. Similar results can be achieved from 24-co. model and 28-co. model.

When the excitation amplitude is large enough, the latter diagonal elements of the coefficients matrix will become larger, stable nonlinear coefficients can be received from nonlinear models (Figs. 8 and 9).

Moreover, Eq. (10) (corresponding to 24-co. model, the coefficient matrix is 12×12) has the smallest condition number among these three equations. This is the reason why it is 24-co. model rather than the other two models that can receive much more stable second-order oil-film coefficients in the case of ordinary excitation amplitude.

5. Conclusions

The results presented here support the following general conclusions:

1. Only when the excitation amplitude is small, the oil-film forces of journal bearing can be assumed as linear one; when the excitation amplitude is large, the oil-film forces are nonlinear. Three nonlinear models (24-co., 28-co. and 36-co. models) are feasible to describe the oil-film forces.
2. When the excitation amplitude is large, the identified linear oil-film coefficients from these three nonlinear models are consistent and close to each other. Reliable linear oil-film coefficients can be obtained through these three nonlinear models.
3. It is difficult to obtain reliable nonlinear oil-film coefficients. The 24-co. model can receive much more reliable second-order oil-film coefficients compared with the other two nonlinear models. However, the other nonlinear coefficients cannot be reliably obtained from these nonlinear models unless the excitation amplitude is large enough.

Acknowledgements

The supports from the National Natural Science Foundation of China (Grant No. 90210007 and 50335030) and China 863 High Tech Project (2002AA412410) are gratefully acknowledged.

References

[1] J.W. Lund, Review of the concept for dynamic coefficients for fluid film journal bearings, *Journal of Tribology* 109 (1987) 37–41.

[2] Z.L. Qiu, A.K. Tieu, The effect of perturbation amplitudes on eight force coefficients of journal bearing, *Tribology Transactions* 39 (1996) 469–475.

[3] H. Hattori, Dynamic analysis of a rotor-journal bearing system with large dynamic loads (stiffness and damping coefficient variations in bearing oil films), *JSME International Journal Series C* 36 (2) (1993) 251–257.

[4] C.M. Muller-Karger, A.L. Granados, Non-linear mdel for stiffness and damping coefficients of hydrodynamic bearing using the minimum square method, *Third International Congress on Numerical Methods in Engineering and Applied Sciences*, Maerida,Venezuela, 1996, pp. 61–70.

[5] C.M. Muller-Karger, L.E. Barrett, et al., Influence of fluid film nonlinearity on the experimental determination of dynamic stiffness and damping coefficients for three-lobe journal bearings, *Tribology Transactions* 40 (1) (1997) 49–56.

[6] C.S. Chu, K.L. Wood, et al., A nonlinear dynamic model with confidence bounds for hydrodynamic bearings, *Journal of Tribology* 120 (3) (1998) 595–604.

[7] F.K. Choy, M.J. Braun, et al., Nonlinear effects in a plain journal bearing: part 1—analytical study, *Journal of Tribology* 113 (3) (1991) 555–562.

[8] M.J. Braun, F.K. Choy, et al., Nonlinear effects in a plain journal bearing: part 2—results, *Journal of Tribology* 113 (3) (1991) 563–570.

[9] S.X. Zhao, A Study on Nonlinear Dynamic Properties of Journal Bearing, Ph.D. Thesis, Xi'an Jiaotong University, China, 2003.